Mixed State Entanglement:
Manipulating Polarisation-Entangled Photons

R. T. Thew[1] and W. J. Munro[1,2]

[1] Centre for Quantum Computer Technology, University of Queensland,
QLD 4072, Brisbane, Australia

[2] Hewlett Packard Laboratories, Filton Rd, Stoke Gifford, Bristol, BS34 8QZ, UK

(February 1, 2008)

There has been much discussion recently regarding entanglement transformations in terms of local filtering operations and whether the optimal entanglement for an arbitrary two-qubit state could be realised. We introduce an experimentally realisable scheme for manipulating the entanglement of an arbitrary state of two polarisation entangled qubits. This scheme is then used to provide some perspective to the mathematical concepts inherent in this field with respect to a laboratory environment. Specifically, we look at how to extract enhanced entanglement from systems with a fixed rank and in the case where the rank of the density operator for the state can be reduced, show how the state can be made arbitrarily close to a maximally entangled pure state. In this context we also discuss bounds on entanglement in mixed states.

I. INTRODUCTION

Since the foundations of quantum mechanics were laid, one of its most curious, and perhaps defining, features has been entanglement. Historically this has been discussed with regard to questions of nonlocal behaviour of quantum systems, a consequence of the famous EPR paper [1] and subsequent work by Bell [2]. In the past decade the focus has shifted to a more information-theoretic interpretation of entanglement in line with the global effort to understand and eventually build a quantum computer. Quantum computing is not the only avenue that has motivated interest. In more immediate terms, realistic endeavours involve quantum cryptographic schemes, dense coding and teleportation as well as general questions regarding quantum information [3,4]. While the realisation of a quantum computer is a long term goal, these pursuits are motivating an enormous amount of cross-disciplinary collaboration in questioning some of the fundamentals of quantum mechanics, information theory, and how the two are related.

The centerpiece of much of this work is entanglement. Quantifying, generating, distributing and maintaining entanglement make up the cornerstones of an enormous amount of research in quantum information science. A means of manipulating entanglement will be vital in distributing and maintaining entanglement, and photons provide the most realistic and accessible means of achieving this. In this paper we refine an experimentally realisable [5] protocol for manipulating arbitrary states of polarisation entangled photons which we have previously introduced [6]. This scheme has been significantly improved and we provide here extensive analysis of the protocol in the context of entanglement transformations. This scheme specifically targeted mixed states, as experimentally it is unrealistic to consider the system isolated from interactions with the environment. We would also like to connect some of the mathematical concepts regarding entangled mixed states with a more intuitive and realistic experimental proposal. In terms of manipulating a state's entanglement and purity there was a proposal of Kent *et al.* [7] pertaining to the requirements for an optimal entanglement transformation. This is all performed in the context of local filtering operations and in this paper we will show how and why this works in a system using polarisation entangled photons and allowing for imperfect photo-detection.

As only two qubit states are considered, an exact expression for the *Entanglement of Formation* (*EOF*), introduced by Wooters [8], will be used.

The *EOF* is

$$E(C(\rho)) = h\left(\left[1 + \sqrt{1 - C(\rho)^2}\right]/2\right) \qquad (1)$$

where h is the binary entropy function,

$$h(x) = -x\ \log(x) - (1-x)\log(1-x) \qquad (2)$$

This is derived in terms of the spin flip operation

$$\tilde{\rho} = (\sigma_y^A \otimes \sigma_y^B)\rho^*(\sigma_y^A \otimes \sigma_y^B) \qquad (3)$$

where σ_y are Pauli operators and the complex conjugation is taken in the computational basis. From this the Concurrence can be found

$$C(\rho) = \max\{\tilde{\lambda}_1 - \tilde{\lambda}_2 - \tilde{\lambda}_3 - \tilde{\lambda}_4, 0\} \qquad (4)$$

where the square root of the eigenvalues for $\rho\tilde{\rho}$, $\tilde{\lambda}_i$, are sorted into descending order.

The other characteristic that is considered here is the purity of the state and the *von Neumann Entropy* provides a convenient and useful measure. The entropy of the bipartite density matrix, ρ_{AB}, is

$$S(\rho_{AB}) = -\operatorname{Tr}\left[\rho_{AB}\log_4\rho_{AB}\right] = -\sum_{i=1}^{4}\lambda_i\log_4\lambda_i \quad (5)$$

where λ_i are the eigenvalues of ρ_{AB}. In the latter form this is analogous to the classical Shannon entropy. The log to base 4 is used as this is the joint state, and hence in this form returns a normalised entropy ranging from zero, for a pure state, to one for the Identity or totally mixed state.

For a correlated system the entropy of the whole system is less than the entropy of its parts due to the information that is present in the correlations between the two systems. For a maximally entangled pure state $S(\rho_A) = S(\rho_B) = \log(2)$ and $S(\rho_{AB}) = 0$. How the state was prepared cannot be determined by considering measurements on the two subsystems. The correlation in the joint state measurements must be considered.

The characteristics of the entropy for a mixed state, regarding both the joint state and local subsystem, will be useful when discussing state transformations. The entropy provides a key element in discussing bounds on the Hilbert space associated with mixed states in the context of state manipulation in general and the scheme introduced here. These concepts will be discussed primarily in terms of a proposed bound on mixed state entanglement enhancement [7] that requires the subsystem entropies to be maximised.

II. ENTANGLEMENT MANIPULATION USING BEAM SPLITTERS

The entanglement manipulation protocol that is to be introduced here relies on the very simple process of filtering, a method proposed by several people [9–11] as a means of manipulating entangled states. This protocol is conceptually similar to the *Procrustean Method* introduced by Bennett *et al.* [12] which dealt with pure states of entangled spin-half particles, in a very generic way.

Our aim is for two parties, A and B, who are spatially separated, to share the optimal entanglement available. The qubits we consider here are polarisation states, where $|V\rangle, |H\rangle$ correspond to the $|0\rangle, |1\rangle$ states within the standard computational basis.

The schematic in Figure (1) represents the proposed manipulation protocol which will be referred to from here on as the Beam Splitter Protocol. Everything to the left of, and including, the BBO (Beta-Barium-Borate) crystal and decohering elements (DEs) are representative of the source that can supply the initial entangled states that we propose to manipulate. The first Polarising Beam Splitter (PBS) at the input, before the crystal, varies the weighting of a superposition state which is then Down-converted at the Parametric crystal generating pure entangled pairs. The decohering elements, after the crystal, vary the mixedness of the state. The recent advances in the preparation of non-maximally entangled pure [13]

and mixed [14] polarisation-entangled states allows for the consideration of a wide variety of initial states, with high production rates for the entangled photons [15].

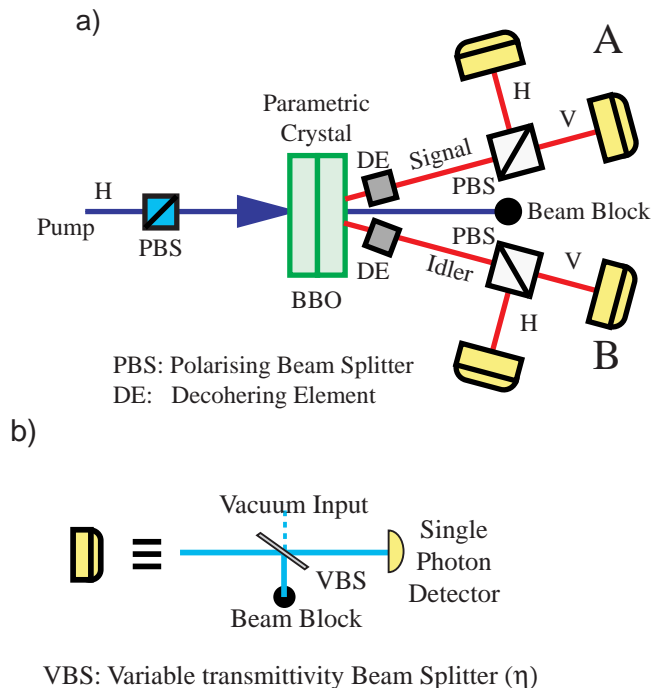VBS: Variable transmittivity Beam Splitter (η)

FIG. 1. The initial polarised beam is incident on a Polarising Beam Splitter (PBS) creating general superposition states which are dependent on the orientation of the PBS. This beam then undergoes a Down-conversion process at the BBO crystal producing pure states where the degree of entanglement is determined from the initial superposition. The Signal and Idler outputs are then subject to independent Decohering Environments (DE) allowing variation in the mixedness of the state. This allows the generation of a wide variety of entangled states. The schematic for the Beam Splitter Protocol illustrates how an entangled state shared between A and B is spatially separated with respect to its polarisation modes by PBSs. Each mode is then incident on another beam splitter with variable transmittivity (VBS). With some prior knowledge of the state the VBSs can be manipulated, concentrating the characteristics of the output state that has coincidence detections at A and B.

The scheme operates in the following manner. The output from the crystal, the two arms labelled *signal* and *idler*, are incident on PBSs, spatially separating the vertical and horizontal polarisation modes of the two separate beams. These modes will be labelled, $|V\rangle_A, |H\rangle_A, |V\rangle_B, |H\rangle_B$. Both the polarisation modes, V and H, in both the arms, A and B, will then be incident on Variable Beam Splitters (VBSs). These variable beam splitters can then be adjusted to obtain the desired output state dependent on the transmission coefficient, η, for each mode. This transmission is polarisation dependent. Due to low detector efficiencies, in this protocol the reflected modes are ignored and the final state that

is considered is the state that has coincidence detections at both A and B. This will be justified shortly.

All four Bell-type states will be considered here. A mixture of two of these non-maximally entangled Bell-type states,

$$|\phi^\pm\rangle_{AB} = \cos\theta_1 |VV\rangle_{AB} \pm \sin\theta_1 |HH\rangle_{AB} \qquad (6)$$

$$|\psi^\pm\rangle_{AB} = \cos\theta_2 |VH\rangle_{AB} \pm \sin\theta_2 |HV\rangle_{AB} \qquad (7)$$

will be used to illustrate the extension from pure to mixed state manipulation. The degree of entanglement in each of these states is determined by the value of θ, i.e. a maximally entangled state will have equal weighting of the coefficients, $\theta_{1,2} = \pi/4$.

When we consider a beam splitter interaction we must also consider that as well as the incident mode, the other port of the beam splitter is subject to the vacuum and similarly the output will also have two modes. The effect that the beam splitters have on a polarisation-entangled state is to transform the modes in the following way

$$|V,H\rangle_{AB}|0\rangle \to \eta_{V,H}|V,H\rangle_{AB}|0\rangle + \sqrt{(1-\eta_{V,H}^2)}|0\rangle_{AB}|1\rangle \quad (8)$$

This can be interpreted as the vertical or horizontal modes being passed by the beam splitter with a probability $\eta_{V,H}^2$, with a component at the reflected port that now has a photon in an ancilla mode with a probability $(1-\eta_{V,H}^2)$. This approach has a similar interpretation to those found by modelling imperfect detectors as a perfect detector plus a beam splitter attenuating the input field [16].

It is easy to determine how a single beam splitter in one arm of the system could be coupled to a specific vertical or horizontal mode. It is not much harder to do this for a beam splitter at A and B, however, we wish to introduce two beam splitters, both vertical and horizontal, to each polarisation arm of the system. This couples a controllable variable, the transmission coefficient, to each mode, where the four variable beam splitters act independently on the four polarisation modes of the bipartite system.

Consider a non-maximally entangled pure state of the form of eq.(7). After interactions with all four of the variable beam splitters, the final state, before anything is discarded, is

$$|\psi\rangle_{tot} = \tilde{\mathcal{N}} \{ \; [\cos\theta \eta_{VA}\eta_{HB}|VH\rangle_{AB}\rangle \pm \sin\theta \eta_{HA}\eta_{VB}|HV\rangle_{AB}]\,|00\rangle$$
$$+ \cos\theta \eta_{VA}\sqrt{(1-\eta_{HB}^2)}\,(|V0\rangle_{AB}|01\rangle + |0H\rangle_{AB}|10\rangle)$$
$$\pm \sin\theta \eta_{HA}\sqrt{(1-\eta_{VB}^2)}\,(|V0\rangle_{AB}|01\rangle + |0H\rangle_{AB}|10\rangle)$$
$$+ \cos\theta\sqrt{(1-\eta_{VA}^2)}\,\sqrt{(1-\eta_{HB}^2)}|00\rangle_{AB}|11\rangle$$
$$\pm \sin\theta\sqrt{(1-\eta_{HA}^2)}\,\sqrt{(1-\eta_{VB}^2)}|00\rangle_{AB}|11\rangle \; \} \quad (9)$$

The modes can be interpreted as those labeled AB being the transmitted modes and the others being the ancilla. Also, for convenience, information regarding the polarisation of the photons in the ancilla modes has been discarded and a simple record of whether there is, or isn't,

a photon in a reflected port at A or B, which is all that is required, has been kept.

It has been remarked previously that due to low detector efficiencies the reflected component is ignored and the state with coincidence detection at A and B is considered. In eq.(9) it can be seen that the only components of the state having coincidence detections at A and B are the two components on the first line. This can be considered to be a coincidence basis state. The coincidence basis state is the state that would have coincidence detections at both A and B, i.e. detections for any of $\{|VV\rangle_{AB}, |VH\rangle_{AB}, |HV\rangle_{AB}, |HH\rangle_{AB}\}$. Alternatively, if it was at all possible to efficiently detect single photons, then perfect single-photon detectors could replace each of the beam blocks in the signal and idler arms in Figure (1b). This would allow the system to operate a gate-like device at the output that, with the aid of classical communication between A and B, was open and letting maximally entangled pairs through as long as a detection is made at one of the previously discarded ports. Again with reference to eq.(9), if this condition was satisfied then the output state to which A and B would have access corresponds to what has been referred to as the coincidence basis state. As perfect photodetection is not a realisable process with current technologies, the beam blocks remain and the state having joint coincidences for A and B is considered. This leaves a reduced output state

$$|\psi\rangle_f = \mathcal{N} \left[\eta_{VA}\eta_{HB}\cos\theta|VH\rangle_{AB} + \eta_{HA}\eta_{VB}\sin\theta|HV\rangle_{AB} \right] \quad (10)$$

with the normalisation

$$\mathcal{N} = \left[\eta_{VA}^2\eta_{HB}^2\cos^2\theta + \eta_{HA}^2\eta_{VB}^2\sin^2\theta \right]^{-1/2} \quad (11)$$

This is a post-selective operation, selecting a subensemble with improved entanglement characteristics and discarding the rest of the ensemble. If no detection is made then the state can be jointly discarded by both A and B. This post-selective process has the advantage that poor detector efficiencies only decrease the coincidence count rate. The requirement for a maximally entangled state is therefore given by

$$\cos^2\theta \; \eta_{VA}^2\eta_{HB}^2 = \sin^2\theta \; \eta_{HA}^2\eta_{VB}^2 \quad (12)$$

If $\cos\theta > \sin\theta$ then either η_{VA} or η_{HB}, or both, can be varied such that $\eta_{VA}^2\eta_{HB}^2 = \tan^2\theta$, thus obtaining a maximally entangled state with probability

$$P = 2\sin^2\theta \quad (13)$$

which constitutes an optimal transformation for single-copy pure states [17,18]. The probability of producing the maximally entangled pure state for this protocol is dependent on the beam splitter transmission coefficients and is determined from the trace of the reduced output state density matrix. This is the probability of obtaining the desired state after the beam splitter settings are determined.

This provides an intuitively simple explanation of this process, for pure states at least, but if mixed states are to be considered then a more convenient representation can be obtained by using the generalised measurement formalism. This procedure constitutes a generalised measurement in that an ancilla is attached to the system, unitary transformations are performed in the extended Hilbert space where measurements are made and then part of the system is traced out and discarded [19].

As we are only interested in the coincidence basis output state, an equivalent local filtering operation can be derived that retains the polarisation coupling characteristics derived for the pure state case. Therefore an *effective* transmission matrix for the joint system can be written

$$(A \otimes B) = \begin{bmatrix} \eta_{VA}\eta_{VB} & 0 & 0 & 0 \\ 0 & \eta_{VA}\eta_{HB} & 0 & 0 \\ 0 & 0 & \eta_{HA}\eta_{VB} & 0 \\ 0 & 0 & 0 & \eta_{HA}\eta_{HB} \end{bmatrix} \quad (14)$$

It can easily be seen that this effective transmission matrix allows for the completely positive mapping of the input state to the coincidence basis output state. The total state transformation matrix is operating in an Hilbert space considerably larger than the original state space, and in this expanded Hilbert space there is now a greater degree of freedom in which to manipulate the state. This is, in part, where the original Procrustean Method obtained its name in that it takes an initial state, places it in an extended Hilbert space, and then manipulates and discards anything not needed.

Thus with all the transmission coefficients acting independently on the $\{|V\rangle_A, |H\rangle_A, |V\rangle_B, |H\rangle_B\}$ modes, the transmission matrix of eq.(14) represents the Beam Splitter manipulation process. This process is analogous to many of the filtering operations that have been proposed [10,11]. Any of the beam splitter transmission coefficients $\eta_{VA}, \eta_{HA}, \eta_{VB}, \eta_{HB}$, can be manipulated individually or in unison. *The key feature of this proposal is that each polarisation mode in A and B can be manipulated independently.* The degree of freedom that this protocol provides means that a wide variety of operations for transforming a bipartite system can be satisfied.

The output state, or more specifically, the reduced *coincidence basis* output state, can now be written in the form

$$\hat{\rho}_{out} = \frac{A \otimes B \ \hat{\rho}_{in} \ A^\dagger \otimes B^\dagger}{\text{Tr}[A \otimes B \ \hat{\rho}_{in} \ A^\dagger \otimes B^\dagger]} \quad (15)$$

This state describes the subensemble that passes the filtering process and would have coincidence detections at A and B. The probability of this state being realised is given by

$$P = \text{Tr}[A \otimes B \ \hat{\rho}_{in} \ A^\dagger \otimes B^\dagger] \quad (16)$$

The only restriction on these operations is that they must satisfy $A^\dagger A \leq I$ and $B^\dagger B \leq I$, being completely positive maps [19].

The case of pure states provided a straightforward example of how this protocol works. So far though, only two of the Bell-type states have been considered. To illustrate the transmission matrix method and cover the other Bell state variants, consider the pure state

$$|\phi^\pm\rangle_{in} = \cos\theta|VV\rangle \pm \sin\theta|HH\rangle \quad (17)$$

This state has the explicit density matrix representation

$$\hat{\rho}_{in} = \begin{bmatrix} \cos^2\theta & 0 & 0 & \pm\cos\theta\sin\theta \\ 0 & 0 & 0 & 0 \\ 0 & 0 & 0 & 0 \\ \pm\cos\theta\sin\theta & 0 & 0 & \sin^2\theta \end{bmatrix} \quad (18)$$

If we apply the Transmission matrix to this state then the output state, given the matrix notation, is

$$\hat{\rho}_{out} = \frac{1}{P} \begin{bmatrix} \eta_{VA}^2\eta_{VB}^2\cos^2\theta & 0 & 0 & \pm\bar{\eta}\cos\theta\sin\theta \\ 0 & 0 & 0 & 0 \\ 0 & 0 & 0 & 0 \\ \pm\bar{\eta}\cos\theta\sin\theta & 0 & 0 & \eta_{HA}^2\eta_{HB}^2\sin^2\theta \end{bmatrix} \quad (19)$$

with $\bar{\eta} = \eta_{VA}\eta_{HA}\eta_{VB}\eta_{HB}$, and the probability is given by the trace of the unnormalised, beam-splitter-transformed, density matrix

$$P = \eta_{VA}^2\eta_{VB}^2\cos^2\theta + \eta_{HA}^2\eta_{HB}^2\sin^2\theta \quad (20)$$

A maximally entangled state is recovered from the coincidence basis output state

$$|\phi^\pm\rangle_{out} = \frac{1}{\sqrt{P}}\left[\eta_{VA}\eta_{VB}\cos\theta|VV\rangle \pm \eta_{HA}\eta_{HB}\sin\theta|HH\rangle\right] \quad (21)$$

providing the requirement for a maximally entangled state

$$\cos\theta \ \eta_{VA}\eta_{VB} = \sin\theta \ \eta_{HA}\eta_{HB}$$

$$\frac{\eta_{VA}\eta_{VB}}{\eta_{HA}\eta_{HB}} = \tan\theta \quad (22)$$

are met. If $\cos\theta > \sin\theta$ then either η_{VA} or η_{VB}, or both, can be varied producing a maximally entangled state with probability $P = 2\sin^2\theta$. Conversely, if $\cos\theta < \sin\theta$ then varying η_{HA} or η_{HB}, would yield a maximally entangled state with probability $P = 2\cos^2\theta$. It could be argued that this constitutes nothing more than a simple variation on the Procrustean Method [12] and requires only filtering at either A or B to distill maximally entangled pure states. The reason for having four individually tunable filters is perhaps not clear yet, and though there is obviously a large degree of freedom in controlling the system, the necessity will become more apparent as the mixed state case is investigated.

III. MIXED STATES MANIPULATION

It is the aim of this section to show how the Beam Splitter Protocol can be extended from pure state manipulation to deal with the more complicated mixed state manipulation. To aid in the understanding of how the protocol can realise this, a state which involves a mixture of two of the non-maximally entangled pure states already discussed will be be introduced. The degree of entanglement of each of the states can be varied as a function of $\theta_{1,2}$ and the mixing of the two will be determined by another parameter γ, such that the state has the density matrix representation

$$\hat{\rho}(\gamma) = \gamma|\phi^+\rangle\langle\phi^+| + (1-\gamma)|\psi^+\rangle\langle\psi^+| \qquad (23)$$

where $|\phi^+\rangle$ and $|\psi^+\rangle$ correspond to positive variants of eq.(6) and eq.(7) respectively. This state will be discussed in terms of the effect that varying the entanglement and mixing of the components has on the entropy and entanglement of the system. In Figure (2) the variation in the entanglement of the system and the entropy of the joint and subsystems is compared as the degree of mixing is varied. This illustrates the result where the entanglement of one of the pure states is not at a maximum and we see that the entanglement of the joint state decreases as the mixing is increased, with $\gamma = 0$ corresponding to the maximally entangled pure state and $\gamma = 1$ the non-maximally entangled pure state. When the state is not maximally entangled the subsystems are not totally mixed and hence the system tends towards the maximally entangled pure state characteristics as the subsystem entropies tend towards $\log(2)$, as γ goes to zero.
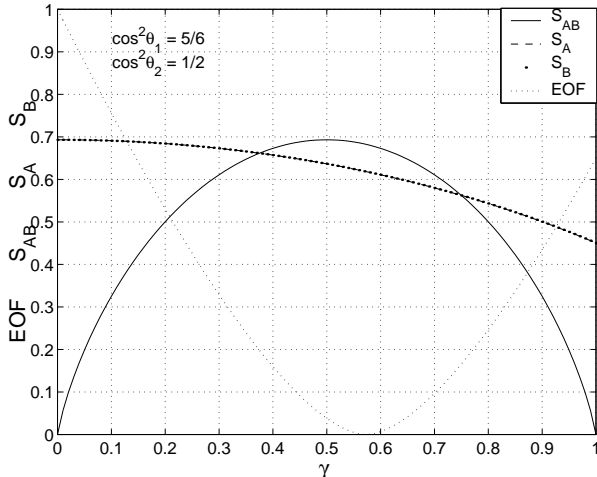
FIG. 2. The EOF and Entropy, for the joint state and local subsystems, as the degree of mixing, γ, is varied. The entanglement decreases as the mixing increases, as expected, between a maximally entangled state, $\gamma = 0$ and a non-maximally entangled state, $\gamma = 1$. The subsystem entropies are equal and reach a maximum of $\log(2)$ at $\gamma = 0$.

Figure (3) illustrates where the entropy of the subsystems are not always equal and how the entanglement peaks when the two subsystem entropies are both equal. The two turning points where the entanglement goes to zero correspond to separable points, analogous to the case of equal mixtures of maximally entangled components, where the entanglement switches from a reliance on one entangled component to the other.

Already a great deal of complexity can be seen to be emerging from a consideration of the entanglement and entropy characteristics of a relatively simple system involving two polarisation-entangled qubits. This is before the extended Hilbert space is introduced via the Beam Splitter Protocol which itself introduces four new variables and hence a higher degree of complexity again.

For pure states the question of optimality of an entanglement transformation for single-copy bipartite states is known. If optimality of mixed states is taken as the most entanglement that can be realised from a state regardless of the joint state entropy, then the conditions to obtain this can be found by looking at the local density matrices of A and B. The local density matrices are found by tracing over the degrees of freedom for the other subsystem, $\rho_A = \text{Tr}_B[\rho_{AB}]$ and $\rho_B = \text{Tr}_A[\rho_{AB}]$. In terms of this, the condition for a Bell diagonal, optimally entangled, state is that $\rho_A = \rho_B = I_2$, corresponding to totally mixed, or random, local density matrices with a maximum amount of entropy, a condition proposed by Kent *et al.* [7].
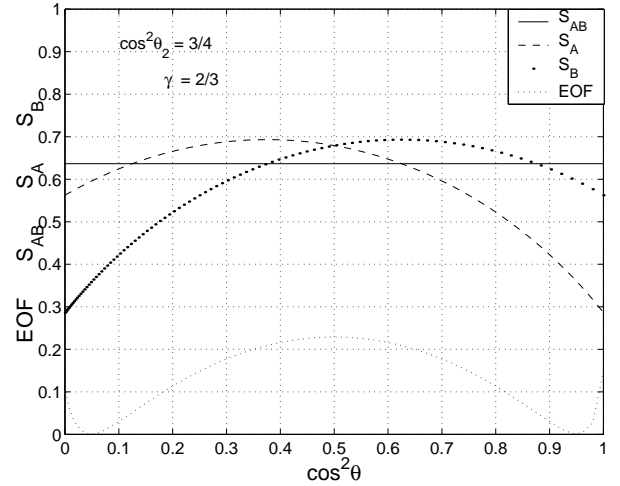
FIG. 3. The EOF, and Entropy, for the joint state and local subsystems, as the degree of entanglement of one of the pure state components is varied, for a fixed degree of mixing. In this instance the subsystem entropies are not always equal, however where they are corresponds to the point of maximal entanglement for the joint state.

How do the entanglement-entropy characteristics for the state vary under the influence of the Beam Splitter Protocol? In Figure (4) the characteristics of a range of states that are obtainable, using the Beam Splitter Pro-

tocol, for a given initial state are plotted. A state of the form of eq.(23) is employed as this can be varied with respect to the mixture and the degree of entanglement of the two pure-state components, which have already been considered. The data points marked with a circle indicate the entanglement-entropy characteristics of the initial state and the solid lines represent a range of states that can be accessed by varying the beam splitters. The two figures are for a range of initial states determined by the mixing parameter, γ, which is labeled on each curve. The degree of entanglement of one component is reduced below that of a maximally entangled pure state.

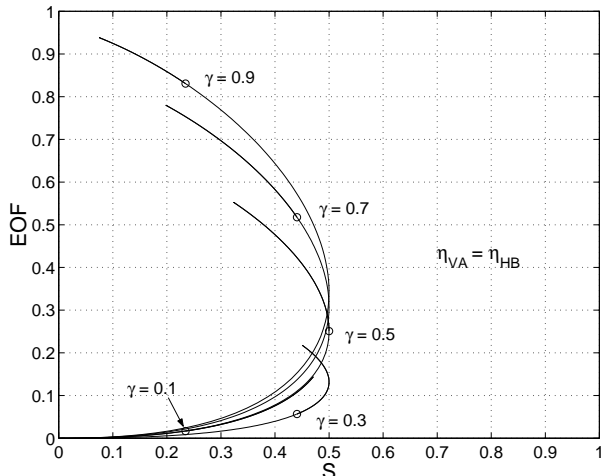
FIG. 4. This figure shows the EOF as a function of the entropy, S, of the joint state, for a range of states of the form of eq.(23), with variation dependent on the mixing and the entanglement of the components. These involve a mixture of a maximally entangled state and one that is weighted towards the $|VH\rangle$ modes. The circles indicate the characteristics for the initial state and the solid line indicates the range of state characteristics obtainable by varying two beam splitters in unison. As the bean splitter transmission is reduced, the curve traces out the Concentration characteristics of the state until the maximum entanglement is reached and the characteristics retrace their path and approach the zero point.

Consider the case of $\gamma = 0.7$ in Figure (4). This state has a mixing which is weighted slightly towards the maximally entangled component, and the other component has only a small degree of entanglement. It is the modes with higher probability of being realised in the less entangled component that are targeted by the Beam Splitter Protocol, η_{VA} and η_{HB}, and hence the mixed state tends towards the maximally entangled pure state component. The maximally entangled component is never fully extracted in this instance as a result of the problem inherent in most mixed state manipulation protocols in that the transformations affect all components of the mixture, not just the component that needs to be removed.

This protocol relies on a certain amount of *prior knowledge* of the state. This knowledge helps determine the required parameters to concentrate the state characteristics. We consider concentration as increasing both the entanglement and purity of a state [6]. Recent advances in quantum state Tomography [13] allow for the measurement and reconstruction of the complete density matrix for a bipartite state, allowing before and after comparisons.

So far the manipulation protocol has been introduced and shown to work for pure states, and it has also been shown to increase both the entanglement and purity of a state consisting of a mixture of pure states, one nonmaximally entangled and another maximally entangled. The pure state transformations have been shown to be optimal, both in the sense that the most amount of entanglement is obtained by the transformation and the transformation is carried out with an optimal efficiency. Can this be extended to arbitrary mixed states? How this protocol works will constitute the majority of the next section, where this state, as well as a range of other states, will be considered and an attempt made to extrapolate some of the results to general systems. Chiefly, the beam splitter dependence on the joint state and the subsystems will be examined in greater detail to determine whether a state can be transformed, and if it can, what beam splitters need to be varied, and by how much, to obtain the most amount of entanglement for the state.

IV. ANALYSING MIXED STATES

The main focus of this paper is the Polarising Beam Splitter Protocol and mixed state entanglement, however, one of the reasons for actually wanting such a device lies in its ability to explore mixed-state Hilbert space. To further illustrate the capabilities of the protocol and at the same time investigate some recent proposals concerning entanglement and various concepts and bounds, a few states will be discussed in detail. To describe the manipulations of a state and look at questions regarding optimality and how these manipulations can be realised, it will be necessary to look at the eigenvalues for the joint system and local subsystems. In this section a more detailed investigation into the mixed state already introduced will firstly take place. The second state that will be looked at will be the Werner state and then finally a state that is a mixture of a pure entangled state and a separable component will be introduced and discussed with a view to determining a bound on the entanglement-entropy plane. A parameterised density matrix will finally evolve from this, and then the Beam Splitter Protocol and the state manipulations will be discussed again in the context of this bound.

6

A. Two Bell State Mixture

Consider again the state consisting of a mixture of two Bell-like states

$$\hat{\rho}(\gamma) = \gamma|\phi^+\rangle\langle\phi^+| + (1-\gamma)|\psi^+\rangle\langle\psi^+| \qquad (24)$$

which has the explicit density matrix after the beam splitter interaction of

$$\tilde{\rho} = \frac{1}{P_B}\left[\gamma \begin{pmatrix} \eta_{VA}^2\eta_{VB}^2\cos^2\theta_1 & 0 & 0 & \bar{\eta}\cos\theta_1\sin\theta_1 \\ 0 & 0 & 0 & 0 \\ 0 & 0 & 0 & 0 \\ \bar{\eta}\cos\theta_1\sin\theta_1 & 0 & 0 & \eta_{HA}^2\eta_{HB}^2\sin^2\theta_1 \end{pmatrix} \right.$$
$$\left. + (1-\gamma)\begin{pmatrix} 0 & 0 & 0 & 0 \\ 0 & \eta_{VA}^2\eta_{HB}^2\cos^2\theta_2 & \bar{\eta}\cos\theta_2\sin\theta_2 & 0 \\ 0 & \bar{\eta}\cos\theta_2\sin\theta_2 & \eta_{HA}^2\eta_{VB}^2\sin^2\theta_2 & 0 \\ 0 & 0 & 0 & 0 \end{pmatrix} \right] \quad (25)$$

with $\bar{\eta} = \eta_{VA}\eta_{HA}\eta_{VB}\eta_{HB}$ as previously, and where

$$P_B = \gamma\left[\eta_{VA}^2\eta_{VB}^2\cos^2\theta_1 + \eta_{HA}^2\eta_{HB}^2\sin^2\theta_1\right]$$
$$+ (1-\gamma)\left[\eta_{VA}^2\eta_{HB}^2\cos^2\theta_2 + \eta_{HA}^2\eta_{VB}^2\sin^2\theta_2\right] \quad (26)$$

To determine the conditions to optimise the entanglement, the reduced density operators for each of the subsystems need to be found. If the subsystem entropies are to be maximised, $S_A = S_B = \log(2)$, then the following constraints must be satisfied

$$\tan\theta_1 = \frac{\eta_{VA}\eta_{VB}}{\eta_{HA}\eta_{HB}} \qquad (27)$$

$$\tan\theta_2 = \frac{\eta_{VA}\eta_{HB}}{\eta_{HA}\eta_{VB}} \qquad (28)$$

As both the Entanglement of Formation and the Entropy are dependent on the eigenvalues of the system, it is beneficial to determine how these behave with regard to the subsystem constraints.

In satisfying the constraints on the local systems, the eigenvalues for the joint system simplify to

$$\lambda_1 = 2\gamma\eta_{VA}^2\eta_{VB}^2\cos^2\theta_1\frac{1}{P_B} \qquad (29)$$

$$\lambda_2 = 2(1-\gamma)\eta_{VA}^2\eta_{HB}^2\cos^2\theta_2\frac{1}{P_B} \qquad (30)$$

Given this, consider the ratio of these eigenvalues:

$$\frac{\lambda_1}{\lambda_2} = \left(\frac{\gamma}{1-\gamma}\right)\frac{\sin 2\theta_1}{\sin 2\theta_2} \qquad (31)$$

Note that this ratio is independent of any transmission coefficients only when the subsystem constraints are satisfied. Thus by satisfying the subsystem constraints, the joint system requirements are also being realised in that the degree of mixing of the state is reduced as much as possible, given the parameters governing the initial state.

When this ratio equals one, the joint system is maximally mixed and there is no entanglement present. Recall Figure (2), the entanglement minima corresponds to the point where $\lambda_1/\lambda_2 = 1$. For a maximally entangled state this is at $\gamma = 1/2$ but if $\theta \neq \pi/4$, then the minima will be appropriately shifted. Which one of the joint state eigenvalues will dominate is determined by both the mixing and the entanglement of the pure state components in the original mixture.

These constraints govern how much the state can be improved by the beam splitters. In general, the entanglement of a state is reduced as the degree of mixing is increased, and this provides a bound on the possible transformations for the state. By satisfying the local system constraints proposed by Kent *et al.* [7], regarding optimal entanglement enhancement, the joint state eigenvalues obtain their optimal value.

B. Werner State

The Werner state can be considered as a weighted mixture of all four of the Bell states [20], a straightforward extension of the mixture of two Bell states just discussed. However, we consider the Werner state, in the form

$$\hat{\rho}_w(\gamma) = (1-\gamma)\frac{I_4}{4} + \gamma\,|\phi^+\rangle\langle\phi^+| \qquad (32)$$

where the initial state, $|\phi^+\rangle$, has a probability γ of being transmitted without errors and there is a component $(1-\gamma)$ of a totally mixed state. In the case where $\gamma \leq 1/3$ the state is separable and as such has no entanglement to recover or maintain. If the pure state component of this mixture is maximally entangled then $S_A = S_B = \log(2)$ regardless of the degree of mixing and the state is as entangled as it can be. It is, perhaps, this characteristic that suggested it might provide a bound on how entangled a mixed state could be. If, however, the pure state component is not maximally entangled, this constraint does not hold.

If the Beam Splitter Protocol is now implemented on a Werner state, with a non-maximally entangled pure state component, then the constraints on the subsystem and joint state eigenvalues are determined, as in the case of the mixture of two Bell states previously. Firstly the subsystems are considered and the constraints that maximise the subsystem entropies are determined. The requirement for the local density matrices of the Werner state, post-beam splitters, to satisfy $S_A = S_B = \log(2)$ are

$$\eta_{VA} = \eta_{VB}, \qquad \eta_{HA} = \eta_{HB} \qquad (33)$$

$$\text{and} \qquad \tan\theta = \frac{\eta_{VA}^2}{\eta_{HA}^2} \qquad (34)$$

The joint system for the Werner state has four eigenvalues, which can be simplified using the previous constraints, and the ratios of the eigenvalues are again independent of the beam splitter coefficients, when the subsystem constraints are satisfied.

So, if the subsystem entropies can be made to equal $\log(2)$, the degree of mixing in the joint state is minimised with respect to the maximum amount of entanglement. Also, as there is no means of removing any of the eigenvalues, a relatively high degree of mixing will be inherent in the system even after the Beam Splitter Protocol. This mixing will however be the minimum obtainable while maintaining $S_A = S_B = \log(2)$. Immediately it can be seen, given the constraints of eq.(33) and eq.(34), that if $\tan \theta \leq 1$, then by setting $\eta_{HA}^2 = \eta_{HB}^2 = 1$ and $\eta_{VA}^2 = \eta_{VB}^2 = \tan \theta$, the mixing and entanglement are optimised.

In Figure (5) the entropies and the entanglement of the state are plotted as a function of the two transmission coefficients, η_{VA} and η_{VB}. These two beam splitters are varied in unison, $\eta^2 \equiv \eta_{VA}\eta_{VB} = \eta_{VA}^2$, to satisfy the constraints on the subsystems. Given this, the entanglement of the state is maximised at the point where the entropy of the local subsystems reaches a maximum, $\log(2)$. The probability of the state with these characteristics being realised is also shown. When the state is as entangled as it can be (here an increase of around 20% is shown) it can be seen that the probability of obtaining this state is around 55%.
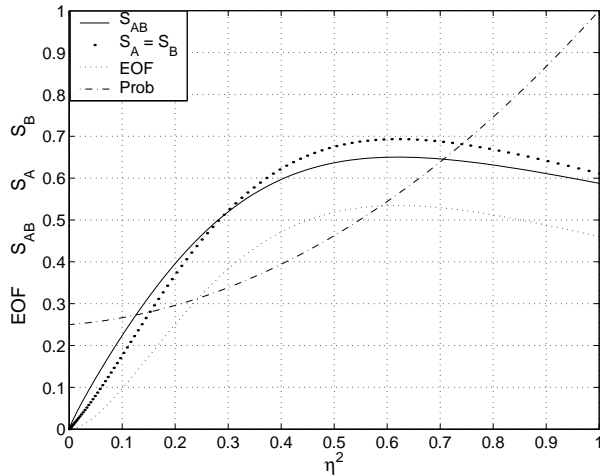
FIG. 5. The variation of the entanglement and entropies, of joint and subsystems, for the Werner state, and the Probability of obtaining these characteristics as two beam splitters are varied in unison, $\eta^2 \equiv \eta_{VA}\eta_{VB} = \eta_{VA}^2$.

The variation in the entanglement-entropy characteristics, Figure (6), shows the results of individually varying the beam splitters, and the improvement that is achieved when they are varied in tandem. η_{VA} and η_{VB}, when varied individually, increase the entropy at the cost of entanglement, but when varied in unison the increase in the entanglement is greater. The maximum entangle-

ment in Figure (6) again corresponds to the point where $\eta_{VA}^2 = \eta_{VB}^2 = \tan \theta \approx 0.6$.

A boundary curve has been introduced in Figure (6) (dotted line) onto the characteristic plane denoting the bound alluded to earlier for the Werner state, where the pure state component is maximally entangled. The curve denotes the characteristics as the γ is varied. Regardless of whether the manipulations are made, individually or in unison, and how many beam splitters are utilised, the entanglement does not exceed this bound.
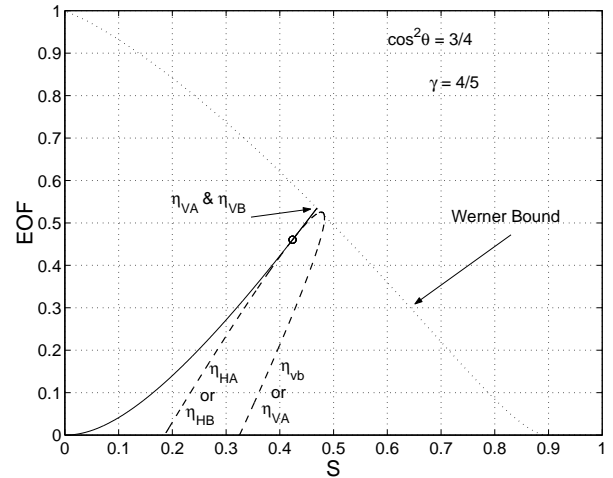
FIG. 6. The EOF and the entropy of the joint system are shown for a range of Werner states, when the beam splitters are varied individually and in unison. The peak value on the bounding curve corresponds to the tuning parameters from Figure (6) where $S_A = S_B = \log(2)$.

C. Entangled + Separable

In the preceding sections, discussion has revolved around mixtures of pure non-maximally entangled Bell states. The first, a mixture of two, and the second, a mixture of all four, and the behaviour of the characteristics of the state under the Beam Splitter Protocol have been observed. To observe the behaviour of a different class of state, a mixture of an entangled pure state and a separable state will now be considered, with the mixture having the form

$$\hat{\rho}_{es}(\gamma) = \gamma \, |\psi^+\rangle\langle\psi^+| + (1-\gamma)|VV\rangle\langle VV| \qquad (35)$$

There are only two eigenvalues for the joint system, $\lambda_1 = \gamma$, $\lambda_2 = (1 - \gamma)$, independent of θ, however, the eigenvalues for the subsystems are dependent on both the mixing and the entanglement of the entangled component.

After the beam splitters, the eigenvalues for the subsystem and the constraints on the joint system are determined, resulting in two requirements, the first being that

$$\tan^2\theta = \frac{\eta_{VA}^2 \eta_{HB}^2}{\eta_{HA}^2 \eta_{VB}^2} \tag{36}$$

which is very similar to those constraints found for previous states. The second constraint poses an interesting problem, or perhaps it should be considered a feature. The second constraint requires that

$$\eta_{VA}^2 \eta_{VB}^2 \to 0 \tag{37}$$

This implies that the subsystems are totally mixed only in the limit of no transmission. Previously, when the subsystem constraints were enforced on the joint system eigenvalues, the degree of mixing for the joint state had been minimised. In this instance the ratio of the eigenvalues is still dependent on the beam splitter transmission coefficients. As such, there is considerable control over the mixing of the state. This state falls in to the class of state that was recently shown by Verstraete et $al.$ [21] that could be brought arbitrarily close to a Bell state by reducing the rank of the density operator.

The behaviour and the entanglement-entropy characteristics of this state, as the beam splitters are varied, is illustrated in Figure (7). The figure highlights the effects that both of these constraints have on the state characteristics.
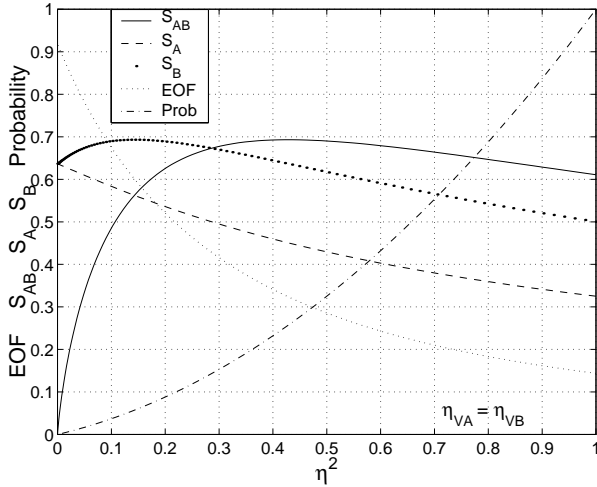

FIG. 7. The entanglement and entropy characteristics for a mixture of non-maximally entangled and separable components as the two beam splitters coefficients are varied with both equal ($\eta^2 \equiv \eta_{VA}\eta_{VB} = \eta_{VA}^2$). The subsystem entropies are not equal except in the limit where the joint state entropy initially increases and only decreasing as the transmission coefficients tend to zero. The pure non-maximally entangled state characteristics are obtained in the limit as the transmission goes to zero.

The mixture consists of $\gamma = 0.3$ of the entangled component and shows the results in the case where the two beam splitters are varied together, $\eta_{VA} = \eta_{VB}$. With these parameter settings the entropies of the subsystems are not equal, $S_A \neq S_B$, and only in the limit as the

transmission coefficients both go to zero do they converge, satisfying eq.(37), and when they do, they are not a maximum and hence the state is not maximally entangled.

If the first constraint, eq.(36), is satisfied and the transmission coefficients of the beam splitters are varied as $\eta_{VA} = \eta_{VB}\tan\theta$, ($\tan\theta \leq 1$) then the behaviour is not that different from this case, except that the subsystem entropies are equal throughout the variation of the beam splitters and in the limit as the transmission tends to zero, the maximally entangled pure state characteristics are approached as $S_A = S_B$ approaches $\log(2)$. As this is achieved, the probability of obtaining these state characteristics tends to zero.

In Figure (8) the state is again considered and the behaviour of the characteristics on the entanglement-entropy plane examined. The dashed curve denotes the behaviour as the beam splitters are varied in tandem as in Figure (7), showing the pure but non-maximally entangled state characteristics being approached. The solid line shows the transformed states obtained by varying the beam splitters while satisfying both the subsystem constraints. This curve shown doesn't pass through the circle marking the initial state characteristics, due to the fact that the initial state, numerically considered, has some η dependence such that initial $\eta \neq 1$, again due to the first constraint.
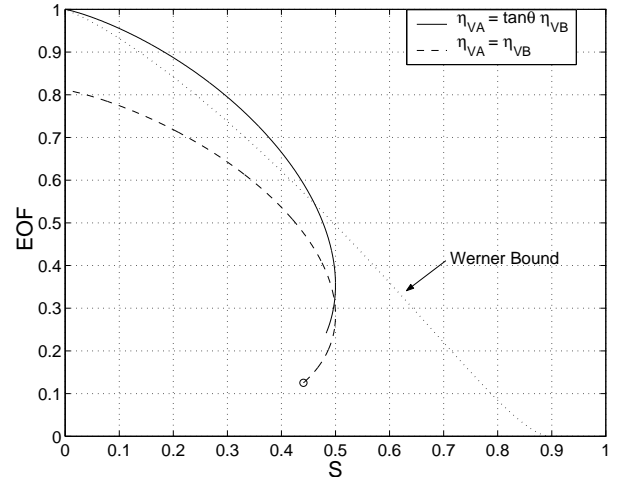

FIG. 8. The range of state characteristics obtainable by implementing the Beam Splitter Protocol on a mixture of entangled and separable states. The two curves, dashed and solid respectively denote varying the beam splitters equally, and when the subsystem constraints are satisfied. The latter case shows that the characteristics can approach those of a maximally entangled state. The Werner state bound is also shown and is crossed for some of the states obtained.

This state has already presented some quite unusual characteristics, however it can also be noted that for variations in the mixture and entanglement of this state, the same concentration characteristics as in Figure (8) are

produced. In fact, this solid curve can be further extrapolated down the plane, for as long as there is some component of the entangled pure state present in the mixture, a state arbitrarily close to a maximally entangled state can be recovered. The probability of such a situation is proportionally unlikely. In the case of a third of the mixture having entanglement corresponding to a 1/3:2/3, weighting of the entangled pure state components, the probability of a maximally entangled pure state being recovered is of the order of 10^6. Regardless of this, this state would provide an incredibly useful state to construct with a view to experimentally considering questions regarding mixed state quantum information, in that it covers so much of the entanglement-entropy plane.

The characteristics of the Werner state suggested that it might provide a bound on mixed state entanglement. In this figure, in the case where the first subsystem constraint is satisfied, there exist states with characteristics above the Werner bound. Clearly the Werner state does not provide an absolute bound for mixed state entanglement and a higher bound needs to be found.

V. BOUNDS ON ENTANGLEMENT

More recently, an attempt to put a bound on mixed state entanglement has resulted in a proposal by Munro *et al.* [22]. The proposed bound involves a density matrix, not entirely dissimilar to the previous mixture of an entangled and a separable state. By considering a slight variation on this state, which involves placing some restrictions on the density matrix elements, a state of the form

$$\hat{\rho}(\gamma) = \begin{pmatrix} 1 - 2g(\gamma) & 0 & 0 & 0 \\ 0 & g(\gamma) & \gamma/2 & 0 \\ 0 & \gamma/2 & g(\gamma) & 0 \\ 0 & 0 & 0 & 0 \end{pmatrix} \quad (38)$$

is obtained, where $g(\gamma) = \gamma/2$ for $\gamma \geq 2/3$ and $g(\gamma) = 1/3$ for $\gamma < 2/3$.

This state has a maximum amount of entanglement for the degree of purity, in terms of the Linear Entropy where the Linear Entropy [23], $S_L = 1 - P$, is related to the purity of the state, $P = \text{Tr}[\rho^2]$. This is then normalised so that

$$S_L = \frac{4}{3}\left(1 - \text{Tr}[\rho^2]\right) \quad (39)$$

returns a value ranging from 0 for pure states, to 1 for a totally mixed state. This state has very similar behaviour to the previous state for $\gamma \geq 2/3$ but significantly different below this point. For this state there are two non-zero eigenvalues for $\gamma > 2/3$ and three below this point. Note here that γ is not the mixture coefficient as previously defined.

If the subsystem constraints are again considered, the following restriction apply

$$\eta_{VA}^2 \eta_{HB}^2 = \eta_{HA}^2 \eta_{VB}^2 \quad (40)$$

and as before

$$\eta_{VA}^2 \eta_{VB}^2 \to 0 \quad (41)$$

It is the case where $\gamma < 2/3$ that the state has the most significant change in its entanglement-entropy characteristics. Below $\gamma = 2/3$ the behaviour of this bounding state differs markedly from that of the previous state. The emergence of the extra eigenvalue increases the entropy and hence extends the coverage of the bound on the entanglement-entropy plane. As such this would suggest that there is some higher bound with respect to the Entanglement of Formation and entropy above what this state proposes. This might also suggest that if the bound is going to be complete, then at some point the emergence of a bounding state with four eigenvalues may be necessary as the entanglement tends to zero. At this point the Werner state may indeed provide the small entanglement - large mixing bound.
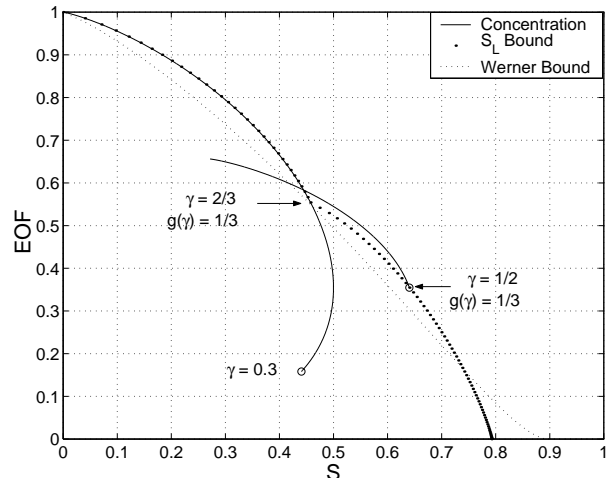

FIG. 9. The *EOF* and entropy characteristics, solid line, for the state given by eq.(35) starting at $\gamma = 0.3$ and the Linear Entropy bound state at $g(\gamma) = 1/2$. The first state has the feature that it approaches and then follows the linear entropy bounding curve up to the peak value. It coincides with the Linear Entropy curve at $\gamma = 2/3$. Both the Werner and linear entropy bounds are shown and the Beam Splitter protocol enables the state characteristics to exceed the Linear Entropy bound. An example of a state starting at $\gamma = 1/2$ is shown.

In Figure (9) the Werner state bound and the Linear Entropy bound are shown, and as just suggested, as the entanglement approaches zero, the Werner state bound is greater, going to zero at $\gamma = 1/3$, $S \sim 0.9$, as the state becomes separable. The previous state is shown again here, where a mixture containing a maximally entangled pure state is used. This state and the Werner State both coincide with the Linear Entropy bound at $\gamma = 2/3$. The

previous state covers quite a large region of this space with the characteristics first increasing in entanglement at the cost of entropy before both the entanglement and the entropy improve, and concentration is realised.

The other curve on this figure to notice is the solid line starting at $\gamma = 1/2$. This curve denotes the characteristics of the Linear Entropy bounding state when the Beam Splitter Protocol is applied to it. Notice that the boundary curve is exceeded, both above and below the bifurcation point for the state at $\gamma = 2/3$. This should not be unexpected, as the subsystem entropies are not maximised for this state. The state was optimised in terms of the Linear Entropy of the joint state. Optimisation in terms of the von Neumann entropy is currently underway.

VI. DISCUSSION

There have been several key points looked at in this paper and all of these have revolved around the Beam Splitter Protocol for manipulating mixed states. In doing this the equivalence between the coincidence detection state and that obtained by a "detect and discard" protocol, with perfect detectors at the reflected ports of the beam splitters, has also been justified. The process was then re-introduced, equivalently, in the context of local filtering operations. Although only a limited range of states were considered, the way the Beam Splitter Protocol transforms a state has shown that, due to the large number of degrees of freedom of the protocol, the scheme is highly adaptable. The transformations have been shown to extract the most amount of entanglement from a state that is possible for a given degree of mixing and in this sense could be considered optimal. The question of a bound on the amount of entanglement that a mixed state can have has been explored, firstly the Werner state and then the Linear Entropy bound.

For mixed states, questions of efficiency and optimality are not clear and as such discussion regarding these have been limited. The distinction is made regarding these concepts - it is one thing for the transformation to obtain the final state with the most amount of entanglement that is possible, and it is another to show the optimal probability or efficiency of carrying out a particular state transformation. The proposed bound on entanglement enhancement of Kent *et al.* [7] applies to the first interpretation and the protocol is shown to satisfy these requirements. In the case of the second interpretation, there has recently been a proposal by Vidal [24] which is an extension of his ideas on single-copy pure states and requires a minimisation over a set of entanglement monotones which has been left for future work.

The primary piece of information to note here is that: IF there is some initial amount of entanglement, AND the subsystems are not BOTH totally mixed, THEN more entanglement can be obtained by transforming the mixed state. The Beam Splitter Protocol introduced here can achieve this, it can do it in a very simple way, and one that is experimentally realisable.

The recovery and maintenance of an entanglement resource is a process that will be of paramount importance for any form of reliable quantum communication. Just as important is the investigation of mixed state entanglement in its own right. An understanding of the relationship between the classical and quantum probability distributions specifying an entangled mixed state is still not complete and any opportunity to investigate this in an experimental regime should be promoted.

The authors would like to thank A.G. White, P.G. Kwiat, K. Nemoto, M. Nielsen and G.J. Milburn for helpful discussions and support. We also thank S. Massar for bringing to our attention ref [21].

1 Electronic address: thew@physics.uq.edu.au
2 Electronic address: billm@hplb.hpl.hp.com
[1] A. Einstein, B. Podolsky, and N. Rosen, Phys. Rev. Lett., **47**, 1215 (1935).
[2] J.S. Bell, Speakable and Unspeakable in Quantum Mechanics, Cambridge University Press, Cambridge, (1987).
[3] J. Preskill, http://theory.caltech.edu/~preskill/ph229/#lecture, (1998).
[4] M.A. Nielsen, and I.L. Chuang, Quantum Computation and Quantum Information, Cambridge University Press, Cambridge, (2000).
[5] P.G. Kwiat, *Private communication*
[6] R.T. Thew and W.J. Munro, Phys. Rev. A, **63**, 030302(R) (2001)
[7] A. Kent, N. Linden and S. Massar, Phys. Rev. Lett., **83**, 2656 (1999)
[8] W.K. Wooters, Phys. Rev. Lett., **80**, 2245 (1998).
[9] S. Popescu, Phys. Rev. Lett. **74**, 2619 (1995).
[10] N. Gisin, Phys. Lett. A. **210**, 151 (1996).
[11] M. Horodecki, P. Horodecki, and R. Horodecki, Phys. Rev. Lett., **78**, 574 (1997).
[12] C.H. Bennett,H.J. Bernstein, S. Popescu, and B.J. Schumacher, Phys. Rev. A, **54**, 3824 (1996).
[13] A.G. White, D.F.V. James, P.H. Eberhard, and P.G. Kwiat, Phys. Rev. Lett. **83**, 3103 (1999).
[14] A.G. White, D.F.V. James, W.J.Munro, and P.G. Kwiat, preprint, (2000).
[15] P.G. Kwiat, E. Waks, A.G. White, I. Appelbaum, and P.H. Eberhard, Phys. Rev. A. **60**, 773 (1999).
[16] D.F. Waals and G.J. Milburn, Quantum Optics, Springer-Verlag, (1994).
[17] H.Lo and S. Popescu, LANL quant-ph/9707038.
[18] G. Vidal, Phys Rev Lett., **83**, 1046 (1999).
[19] M.A. Nielsen, C.C. Caves, B.J. Schumacher, and H. Barnum, LANL quant-ph/9706064.
[20] R.F. Werner, Phys. Rev. A, **40**, 4277 (1989)

[21] F. Verstraete, J. Dehaene and B. De Moor, LANL quant-ph/0011111.

[22] W.J. Munro, D.F.V. James, A.G. White, and P.G. Kwiat, submitted, (2001).

[23] S. Bose, and V. Vedral, LANL quant-ph/9912033

[24] G. Vidal, J. Mod. Opt., **47**, 355, (2000).